

Effect of pores and grain size on the elastic and piezoelectric properties of quartz-based materials†‡

JULIE AUFORT^{1,*}, OKTAY AKTAS¹, MICHAEL A. CARPENTER¹ AND EKHARD K.H. SALJE^{1,*}

¹Department of Earth Sciences, University of Cambridge, Downing Street, Cambridge CB2 3EQ, U.K.

ABSTRACT

The role of grain size and porosity in the piezoelectric and elastic properties of SiO₂-based materials was investigated using resonant piezoelectric spectroscopy (RPS) and resonant ultrasound spectroscopy (RUS). RPS performed on agate revealed a piezoelectric effect comparable in magnitude to that in single-crystal quartz. The observed strong piezoelectricity in agate requires preferential orientation of SiO₂ during crystal growth. Similarly, in novaculite and sandstone finite (but weak) RPS signals were evident, suggesting that the expected randomization of the piezoelectric quartz grains is incomplete. On the other hand, Vycor, a silica glass with a porosity of 40%, showed no evidence of the piezoelectric effect. According to temperature-dependent RPS and RUS measurements, the α - β transition temperature in quartz does not change in polycrystalline samples. Finally, the temperature dependence under heating of the elastic constants is reversible in quartz and agate and irreversible in sandstone and Vycor.

Keywords: Resonant ultrasound spectroscopy, resonant piezoelectric spectroscopy, porosity, SiO₂-based materials, α - β phase transition, piezoelectricity

INTRODUCTION

Many SiO₂-based materials form crystal structures containing SiO₄ tetrahedra that are linked to form three-dimensional frameworks. The most common example is quartz, which displays chirality and is piezoelectric both in the α and β phase. The phase transition is displacive and transforms as the piezoelectric coefficient d_{14} (Salje et al. 1992). The α phase, space group $P3_121$, is piezoelectric with the two active coefficients d_{11} and d_{14} (and their symmetry equivalent parameters). At high temperatures, the transition from the α phase to the (high-temperature) β phase, space group $P6_222$, maintains d_{14} piezoelectricity. The transition $\beta \rightarrow \alpha$ near 847 K is co-elastic with a large decrease of the molar volume and other non-symmetry-breaking spontaneous strains under cooling (Carpenter et al. 1998). The soft mode has B_1 symmetry. There is no bilinear coupling between the strain and the structural order parameter (the tetrahedral tilts), which would be allowed by symmetry. Though the order parameter is two-dimensional, under equilibrium conditions only one component Q_i of the order parameter Q differs from zero in single domain α -quartz. The non-symmetry breaking strains are e_1+e_2 and e_3 , namely the contraction in the plane perpendicular to the crystallographic c -axis and the contraction along the c -axis (Carpenter et al. 1998). All shear spontaneous strains e_i ($i > 3$) are strictly zero.

In contrast to the uniform deformation of a single crystal, phase transitions in granular quartz suffer from non-uniform deformations of adjacent grains. Pertsev and Salje (2000) argued that such differential deformations in close packed materials lead to changes of the phase stability of each phase. In this case, the stepwise transition would be smoothed and the transition temperature would increase. A typical granular SiO₂ material is agate,

where such effects have indeed been seen by Ríos et al. (2001) who measured Q by second harmonic generation (SHG), the temperature evolution of lattice parameters and the transition entropy, and observed these inter-grain effects. Mechanical parameters, such as RUS signals, were measured by McKnight et al. (2008) who found no significant deviations from the behavior of large grain quartz crystals because only those grains that lead to the spanning network of the agate sample determine their mechanical behavior. These grains are not subjected to the deformation of neighboring grains due to the fairly porous nature of agate.

It is the purpose of this article to show that resonant piezoelectric spectroscopy (RPS) measures the mechanical excitations of SiO₂-based materials. The piezoelectric conversion occurs on a local scale and only those local excitations that give rise to mechanical vibrations, are measured. They relate to connecting grains, while isolated grains vibrate locally and do not contribute to the macroscopic mechanical excitation of the entire sample.

The second question concerns the validity of the piezoelectric coupling for smaller grain sizes and even for silica glass. It is already known that quartz is macroscopically piezoelectric while silica glass is not. We show that in samples with smaller grains, such as agate and novaculite, which are both chemically SiO₂, piezoelectric signals are reduced in comparison with quartz. Glassy Vycor, a nanocrystalline form of SiO₂ (Salje et al. 2011), shows no signal while a very weak signal exists in sandstone when SiO₂ grains are cemented by calcite.

We address indirectly the issue of unexpected piezoelectricity in various materials that has been raised previously by Damjanovic and collaborators (Rojac et al. 2012; Vacche et al. 2012; Damjanovic et al. 2012). It has been proposed by Damjanovic (1997) that some piezoelectric effects are due to the existence of domain walls and their weak pinning by defects. The relevant domain boundaries in quartz are Dauphine twin boundaries (Calleja et al. 2001). They are rare and would not

* E-mail: julie.aufort@ens.fr and ekhard@esc.cam.ac.uk

†‡ Open access: Article available to all readers online.

produce significant piezoelectric signals, so that we can rule out this mechanism for SiO₂-based materials. For a review on piezoelectric ceramics that have been poled in an electric field, we refer the reader to Damjanovic (1998). As quartz is piezoelectric but not ferroelectric, no ferroelectric poling is possible. Therefore all polycrystalline samples are unpoled by nature of the crystal structure and, hence, not piezoelectric by symmetry as randomly oriented dipoles should cancel each other out. This is not the case, however, as we will show that some additional “structural poling” or some anisotropic crystal growth is required to explain this effect.

Finally, flexoelectric effects are often invoked for the explanation of piezoelectricity in materials (e.g., Tagantsev and Yurkov 2012). We will show that no piezoelectric properties exist in the extreme case of porous, amorphized SiO₂-based materials with an enormous surface. We hence show that no surface related piezoelectric effects exist in highly porous SiO₂.

EXPERIMENTAL METHODS

Resonant ultrasound spectroscopy (RUS) and resonant piezoelectric spectroscopy (RPS)

The principles of RUS have been described in detail by Migliori and Maynard (2005) and Migliori and Sarrao (1997). RUS is used to measure the resonant frequencies of normal modes of vibration of a material in the frequency region ~0.1–2 MHz. The high-temperature RUS arrangement used for the experiments described here consists of two alumina rods mounted horizontally and has been described by McKnight et al. (2008). As shown in Figure 1, piezoelectric transducers are attached to one end of each rod while the sample is supported across diametrically opposite corners between the other ends that are inside the furnace. An ac voltage is applied across one of the transducers to generate the acoustic signal that is transmitted down the buffer rod and the second transducer acts as the detector for resonances that are excited in the sample and transmitted back along the other rod. The applied voltage for RUS and RPS measurements in this study was 10 V.

Absolute values of the amplitudes of resonance peaks in the RUS spectra are highly variable as they are highly sensitive to the mechanical coupling of the sample with the alumina buffer rod. The peak frequencies, on the other hand, depend on the shape and elastic moduli of the sample. As the geometry hardly changes under heating and cooling we find that RUS is an ideal method to follow the temperature evolution of the relative moduli of a sample where the square of any resonant frequency is proportional to some effective modulus (Migliori

and Maynard 2005). Most resonance modes are dominated by shearing motions of the sample, and the resonance frequencies provide information primarily on the shear modulus, therefore.

Room-temperature RUS spectra of samples of quartz, agate, novaculite, sandstone, and Vycor were measured in the frequency range 100–1000 kHz. Each RUS spectrum collected at high temperature contained 65 000 data points over a frequency range between 200 and 1000 kHz. All the spectra were transferred to the software package Igor Pro (WaveMetrics) for detailed analysis.

RPS could be considered as an electrical analog of RUS, as it involves the application of an ac voltage across the sample (Aktas et al. 2013a, 2013b; Salje et al. 2013). The same experimental arrangement as in RUS is used but the mechanical excitations are stimulated by applying the ac voltage via silver electrodes to two parallel surfaces of the sample, as shown in Figure 1. The applied voltage, 10 V, leads to the oscillation of the matrix and/or domain boundaries through the piezoelectric effect in the sample, which creates macroscopic strain fields proportional to the applied electric field. The resulting elastic wave becomes resonant if the applied field frequency corresponds to one of the mechanical resonance frequencies of the sample. Mechanical resonances are detected using a piezoelectric receiver, as in RUS. Only piezoelectric materials can emit such waves, but the piezoelectric effect need not be macroscopic and can relate to small local regions that deform elastically under an external electric field (Salje et al. 2013).

Room-temperature RPS spectra of quartz, agate, novaculite, and sandstone were measured in the frequency range 100–750 kHz. High-temperature RPS spectra of quartz and agate, each containing 65 000 data points, were collected in the frequency range 200–1000 kHz.

Samples

Agate samples came from Ardownie, Scotland, and their characteristic grain size is 50–90 nm (Ríos et al. 2001). Novaculite, from Arkansas, U.S.A., has a larger grain size of 1–5 μm (Keller et al. 1985). The red sandstone was from Arran, U.K., from the Devonian period and is largely the result of the intrusion and uplift of Tertiary granites (Friend et al. 1963). It belongs to the lithostratigraphic unit of Old Red Sandstone and is of considerable importance to early palaeontology for its fossil content. The main components are 79% quartz, 5% feldspar, 11% clay, the cement consists mainly of carbonates. The average grain size is 0.3 mm.

Vycor is a porous SiO₂-ceramic synthesized via a temperature-induced phase separation of Na₂O-B₂O₃-SiO₂ melt. After cooling, the Ba₂O₃-rich phase is leached out with an acidic solution that leaves a 96% pure SiO₂ skeleton containing cylindrical pores randomly distributed in length, density, and angle. The mean ratio of pore diameter d over pore length l was found to be $d/l \geq 0.232$ (Levitz et al. 1991). Pores of our sample show an average diameter of 7.5 nm and a narrow pore size distribution. Vycor has a non-granular structure constituted of a continuous glass skeleton. The fact that compressive failure strength is expected to depend to a large extent on the adherence between grains (Delenne et al. 2009) explains why the failure strength is much greater in highly connected Vycor than in Sandstone (Salje et al. 2011). The thermal stability of the structures was tested by heating the samples to temperatures well above the phase transition point. Vycor changed at 1230 K while sandstone degraded much earlier when the differential thermal expansion between the matrix and the cement weakened. We will describe these results in the next section.

The quartz, agate, novaculite, and Vycor samples used for RUS had platelet geometry with a thickness of ~1 mm and a surface area varying between 3 × 5 and 5 × 7 mm².

RESULTS

Quartz

Figure 2a shows a stack of RPS spectra collected from the single-crystal sample of quartz, with displacements up the y-axis in proportion to the temperature at which they were collected. All resonance peaks show a frequency minimum at the α-β transition at $T_c = 846$ K. Our RUS observations are in agreement with Carpenter et al. (1998) and McKnight et al. 2008. Quartz shows strong RPS signals compared with other SiO₂-based materials (Fig. 3) similar to agate but much stronger than from novaculite and red sandstone. No RPS signals were observed for Vycor at room temperature. The SHG signal for quartz shows the same trend as RPS (Ríos et al. 2001).

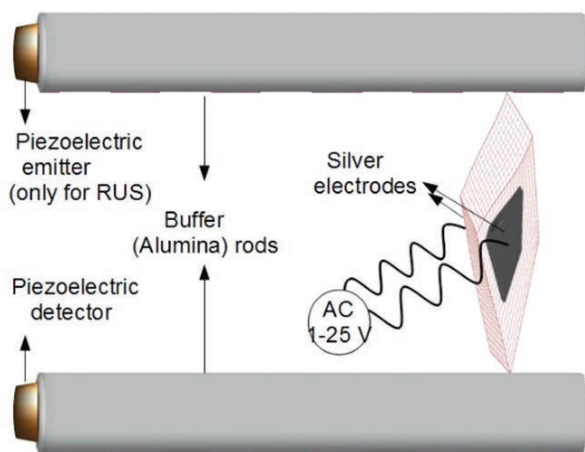


FIGURE 1. Schematic diagram of the experimental arrangement for resonant ultrasound spectroscopy (RUS).

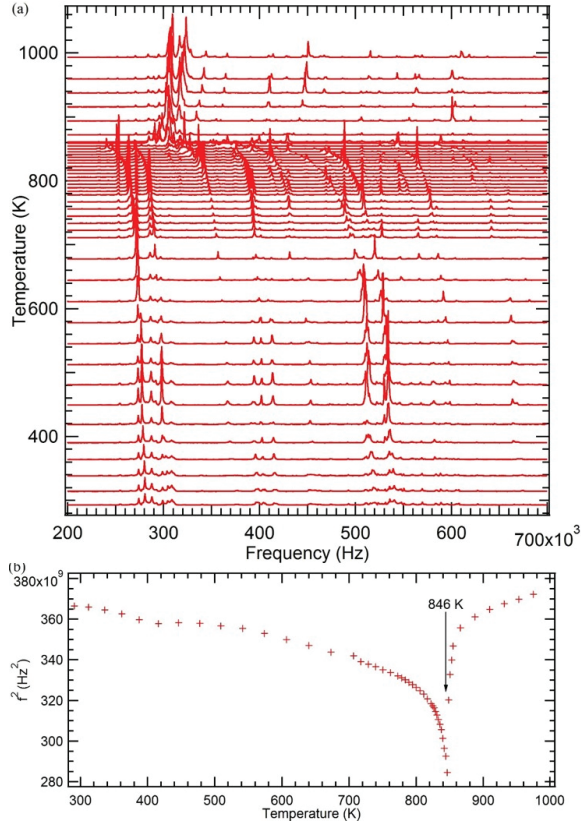


FIGURE 2. (a) RPS spectra for quartz in the frequency region 200–700 kHz at intervals during heating from room temperature up to 993 K. (b) Squared frequency variation for the peak at 600 kHz.

Agate

In agate the RPS resonance frequencies obtained coincide with RUS frequencies (Fig. 4). Figure 5a shows a stack of RPS spectra collected for agate during heating. Resonance frequencies decrease as $T \rightarrow T_c$ from below but, in contrast to quartz, we found no RPS signal above the α - β transition temperature in agate. Figure 5b shows RUS spectra collected for agate during heating. The pattern observed in Figure 5b is similar to that seen for RUS on quartz by McKnight et al. (2008) and RPS on quartz in Figure 2a. Figure 5c shows a minimum in the squared resonant RUS frequencies occurring in the spectrum collected at 844 K (571 °C) and an extinction of the RPS signal at 840 K, a few degrees below the transition temperature of single-crystal quartz.

Figure 6 shows that both RPS and RUS signals suddenly collapse in amplitude at the $\alpha \leftrightarrow \beta$ transition temperature as expected by the high absorption of sliding movements in the incommensurate phase of quartz. The SHG signal for agate at $T > T_c$ decays gradually while RPS disappears abruptly. SHG signals average over all grains, including small grains, while RPS only takes into account larger spanning grains that determine the elastic properties of the sample.

Sandstone

The temperature evolution of elastic resonances in RUS spectra from red sandstone is shown in Figure 7a. All resonances

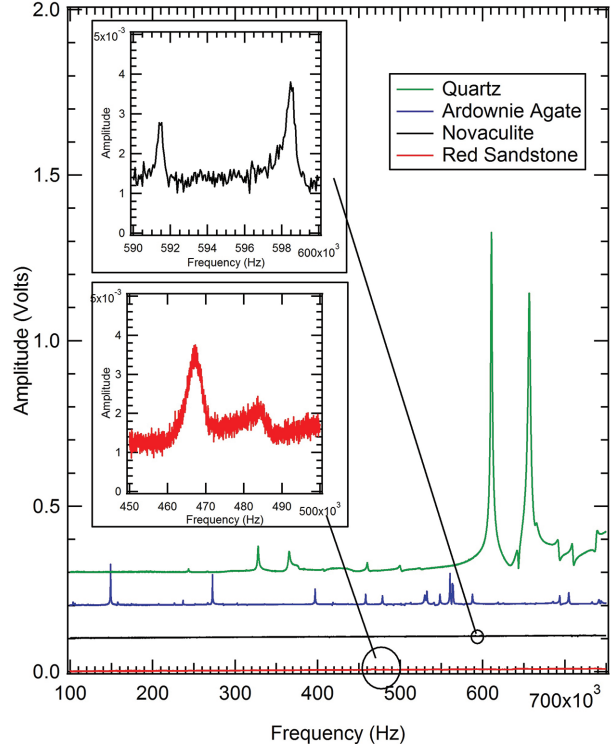


FIGURE 3. Room-temperature RPS spectra of quartz, agate, novaculite, and red sandstone.

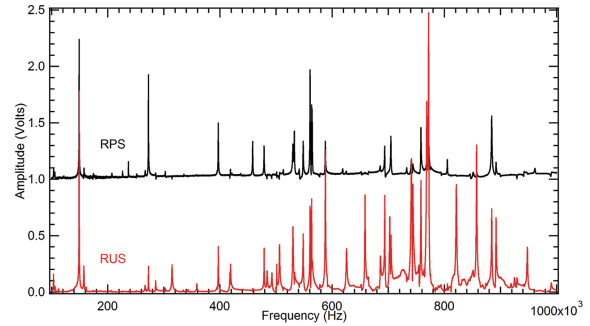


FIGURE 4. Room-temperature RUS and RPS spectra of agate.

show a decrease in frequency from T_c down to room temperature, indicating a stiffening of the elastic constants. In this case, softening with increasing temperature is more pronounced than in agate and quartz, as the shift in frequency is ~ 280 kHz vs. ~ 90 kHz for quartz and ~ 105 kHz for agate. In quartz and agate, the curvature is more pronounced as the transition point is approached. However in sandstone a steep decrease in frequency is first observed at around 400 K. Above T_c all resonances show very little change in frequency. Only at higher temperatures, above 1100 K, a decrease in frequency, e.g., softening of the elastic constants, is observed. This is not similar to the softening above T_c observed in both quartz and agate.

Figure 7b shows the evolution of the resonances during cooling from 1145 K down to room temperature. For quartz and agate, RPS spectra for heating and cooling were similar, as the

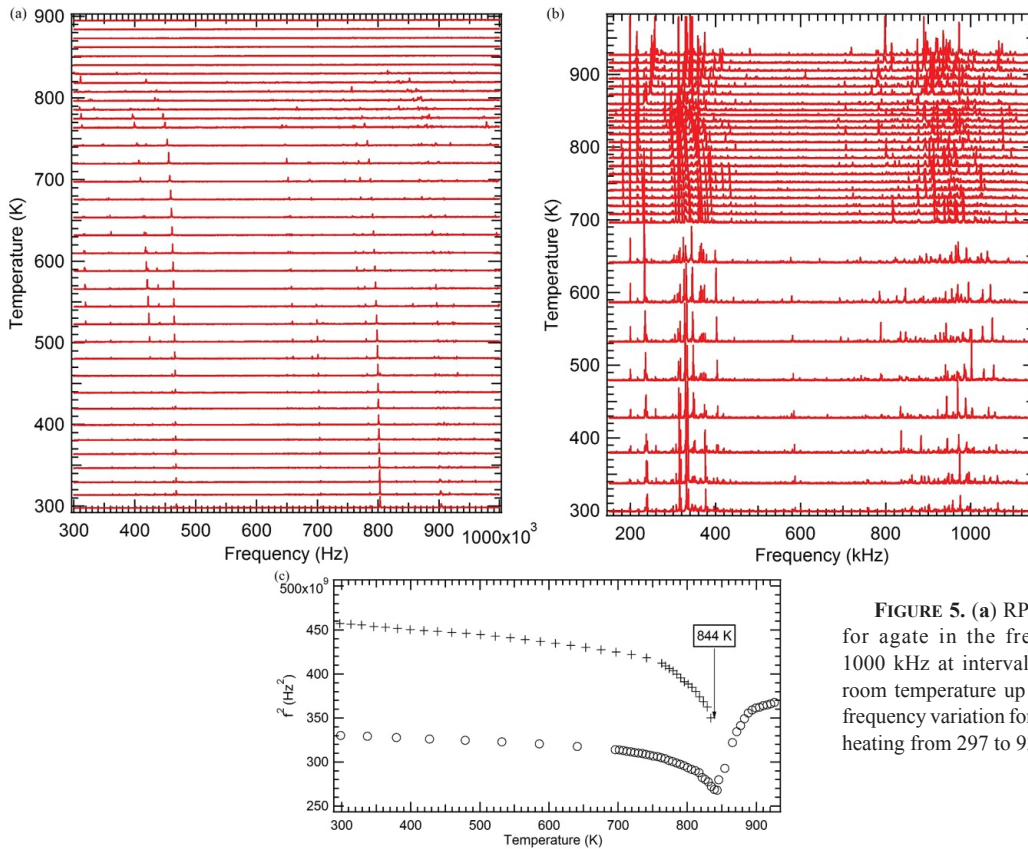


FIGURE 5. (a) RPS and (b) RUS spectra for agate in the frequency region 300–1000 kHz at intervals during heating from room temperature up to 932 K. (c) Squared frequency variation for agate, collected during heating from 297 to 932 K.

temperature dependence of the elastic constants is reversible. In sandstone the temperature dependence of the elastic constants is clearly irreversible, as was found for the quartzite sample of McKnight et al. (2008). The irreversible change is due to microcracking when grains pull apart during the first heating through the transition point. This irreversibility in terms of resonance frequencies is shown in Figure 8c.

Vycor

Figure 8a shows the temperature evolution of elastic resonances in RUS spectra from Vycor. As the temperature rises to 1000 K the resonance frequencies increase. At least part of this stiffening is irreversible, as the higher resonance frequencies are maintained during cooling (Fig. 8b). In contrast to quartz, agate, and sandstone, Vycor shows no anomalies in the vicinity of T_c . When the experiment was repeated and the sample was heated for a second time to 1225 K, the difference between the heating and the cooling is more pronounced than for the first run (Fig. 8c). This is associated with a significant change in microstructure that is clearly visible at a scanning electron microscope scale (Fig. 9).

Finally, we compare in Figure 10 the temperature evolution of squared resonance frequencies in single-crystal quartz, sandstone, Ardornie, Mexican (McKnight et al. 2008), and Brazilian agate (McKnight et al. 2008), and novaculite (McKnight et al. 2008). The frequency minima observed in all samples (except for novaculite) are located near 847 K, indicating that the α - β transition temperature remains the same for all samples. With

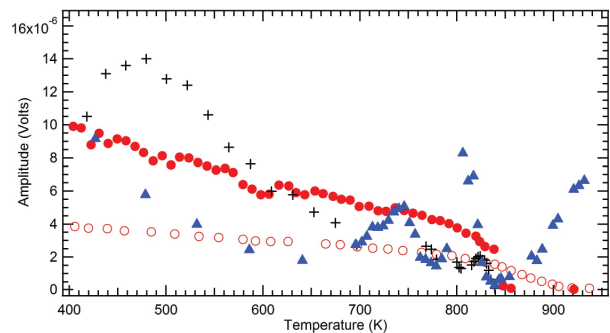


FIGURE 6. Amplitude of RPS (+) and RUS (triangle) signal in agate and excess second harmonic intensity of quartz (solid circle) and nanoquartz (open circle) (Rios et al. 2001) as a function of temperature.

comparison to the variations of the bulk and shear modulus in polycrystalline quartz (Ohno et al. 2006), which are also plotted in Figure 10, one can see that the squared frequency variation in agate is similar to the variation of the bulk modulus in quartz, with a high recovery after the phase transition, revealing that mainly the bulk modulus was captured in agate and not the shear modulus.

DISCUSSION

Quartz is strongly piezoelectric and we find accordingly that the RPS amplitudes are very large. The resonance peaks and their

thermal shift reproduce the temperature evolution of the elastic moduli with a large decay near the α - β phase transition point (Carpenter et al. 1998). In other samples the functional SiO_2 molecular groups, which could give rise to piezoelectricity, are geometrically randomized and one may be tempted to conclude that no RPS signal is expected, besides from small surface effects (Zubko et al. 2013). This is not the case, however. The RPS signals are reduced but not as dramatically as surface effects would imply. In Figure 5a, the RPS amplitudes in agate are comparable with quartz (the largest amplitudes in quartz apart), while novaculite and sandstone show amplitudes reduced by ca. three orders of magnitude. The spectra are still typical for bulk piezoelectricity so we can confirm that the randomization of the piezoelectric effect in these samples does not lead to the complete destruction of polarity. This coincides with observations of polarity in ceramic relaxors by Damjanovic (1998). The orientation of the SiO_2 grains in agate shows a preferential orientation without which we would not see such a strong RPS signal. The observation that Vycor is not piezoelectric shows that even large surfaces are insufficient in SiO_2 to generate piezoelectricity via the flexoelectric effect near surfaces.

We now follow the temperature dependence of the RUS and RPS signals through the α - β phase transition. First, we find that the transition temperature does not change between the samples (except for novaculite, Fig. 10). This observation indicates that

the macroscopic collapse of the structure at the transition point remains the same in all samples with the exception of novaculite (McKnight et al. 2008). In novaculite the transition temperature was 7 K higher than in other samples, suggesting that the array of quartz grains does not fall apart or crack at the transition point and that internal pressure may lead to an increase in the α - β transition temperature.

On a local scale, we have two observations. The second harmonic optical signal, SHG, measured by Rios et al. (2001), shows the same decay at low temperatures as RPS and RUS of agate. At the α - β transition point the macroscopic elastic response collapses while the local optical signal decays gradually with increasing temperature (Fig. 6). This coincides with the prediction of Pertsev and Salje (2000) who showed that small connected grains will show a continuous phase transition and large, spanning grains, which are not closely packed, will show the un-renormalized transition behavior, i.e., a stepwise transition. SHG measures all grains including the small grains while RPS sees only those grains that take part in the spanning of the sample and that define the elastic moduli of the sample. The same argument holds for novaculite, where the grains are not interconnected because the material is porous and local relaxations may be possible. This avoids the squeezing of adjacent grains and hence the renormalization of the Landau potential (Pertsev and Salje 2000).

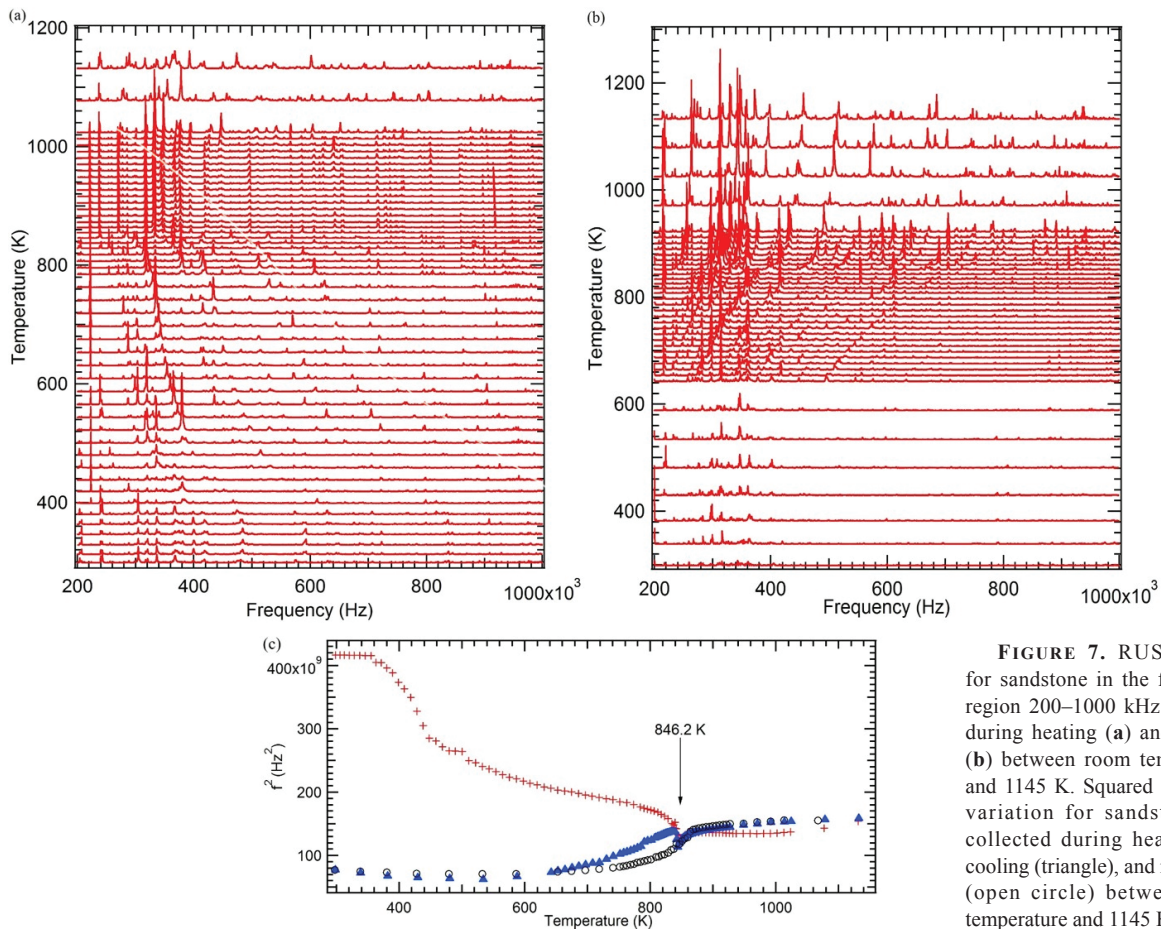


FIGURE 7. RUS spectra for sandstone in the frequency region 200–1000 kHz collected during heating (a) and cooling (b) between room temperature and 1145 K. Squared frequency variation for sandstone (c), collected during heating (+), cooling (triangle), and re-heating (open circle) between room temperature and 1145 K.

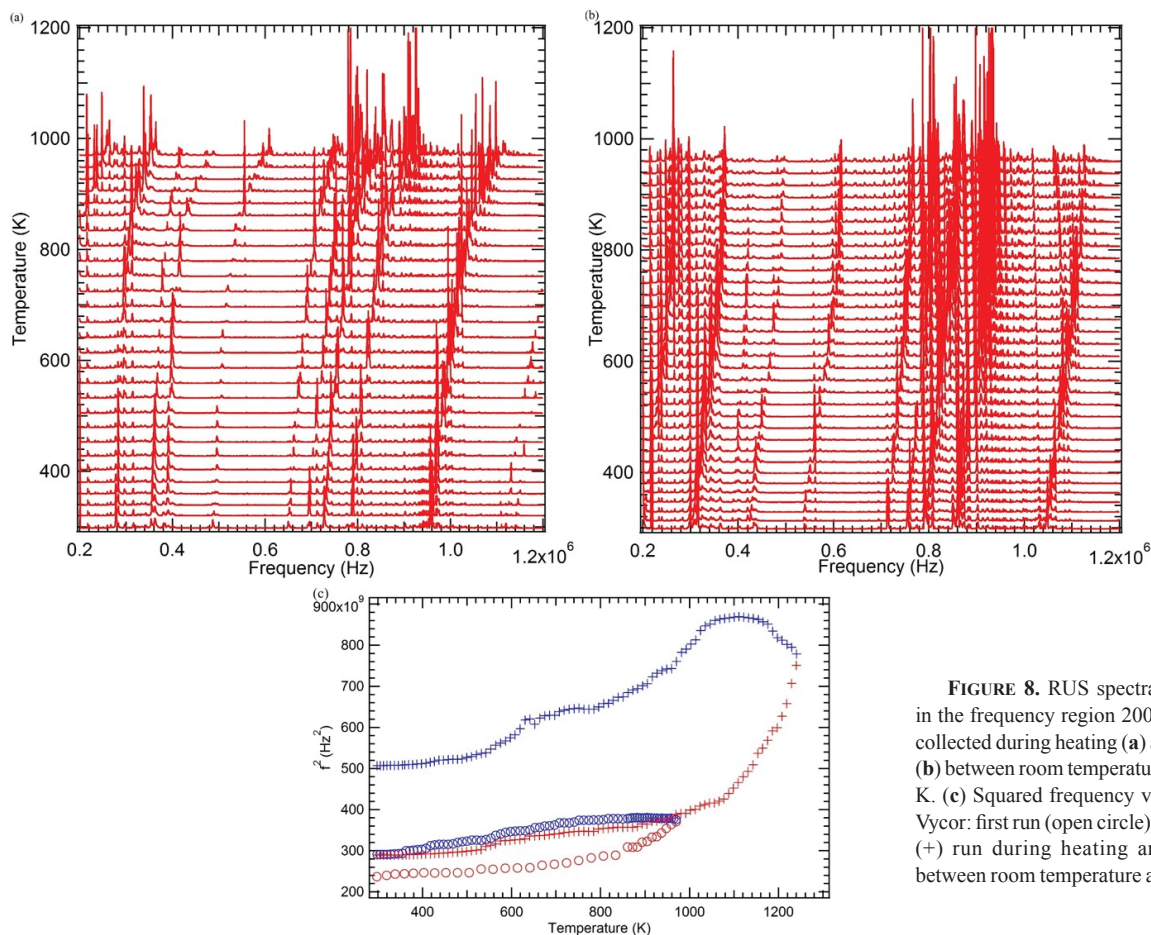


FIGURE 8. RUS spectra for Vycor in the frequency region 200–1200 kHz collected during heating (a) and cooling (b) between room temperature and 1000 K. (c) Squared frequency variation for Vycor: first run (open circle) and second (+) run during heating and cooling between room temperature and 1225 K.

Even higher degrees of porosity are found in Vycor (40% porosity) and sandstone (12% porosity). The grain sizes are particularly small in Vycor with pore diameters of some 7.5 nm. When this material is heated surface melting occurs. This effect is clearly seen in the RUS spectra in Figure 9. The spectra degrade and become irreproducible already at temperatures of some 800 K while full surface melting happens above 1000 K. Melting increases the moduli of the sample by reducing the porosity. The close connection between porosity and the elastic bulk modulus was reviewed in (Salje et al. 2010). A change of porosity from 40% in the initial sample (Salje et al. 2011; Baro et al. 2013) leads to an increase of the moduli by a factor of 4–5 (Salje et al. 2010). The observed increase in the squared resonance frequency, which is proportional to the elastic modulus, by a factor of ca. 2, shows that at 1250 K not all porosity has been destroyed. This is also seen in the micrographs (Fig. 2b), which still shows large holes in the annealed Vycor sample although the struts between the holes are solid without further porous holes.

The temperature evolution of elastic properties in sandstone lies in between the cases of agate and Vycor. The heating and cooling experiments on sandstone lead to irreversible temperature dependences of the moduli. In sandstone, the porosity of the sample is not located in the SiO₂ components of the sample but in between solid SiO₂ grains that are cemented together by carbonates. Heating sandstone leads to stresses between the

quartz grains and the cement. These stresses become largest when the phase transition leads to massive shape changes of the quartz grains. In RUS (Fig. 7), we observe that the sample cracks during the first heating as it bursts by expanding, then what has not been destroyed during heating bursts again by contracting during cooling.

A novel correlation effect is seen in sandstone: the individual quartz grains are piezoelectric but one would assume that the piezoelectric effect vanishes because the grains are randomly oriented. This is not the case because a small but clear RPS signal is observed (Fig. 3). This indicates that the sandstone sample

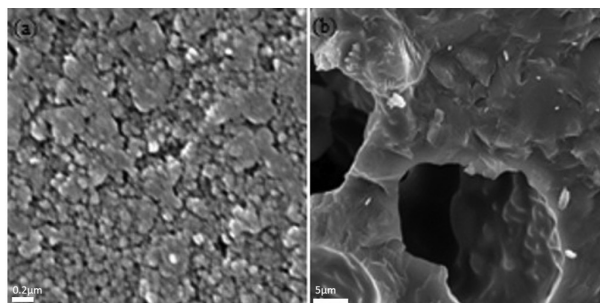


FIGURE 9. SEM pictures of Vycor taken before (a) and after (b) heating the sample at 1200 K.

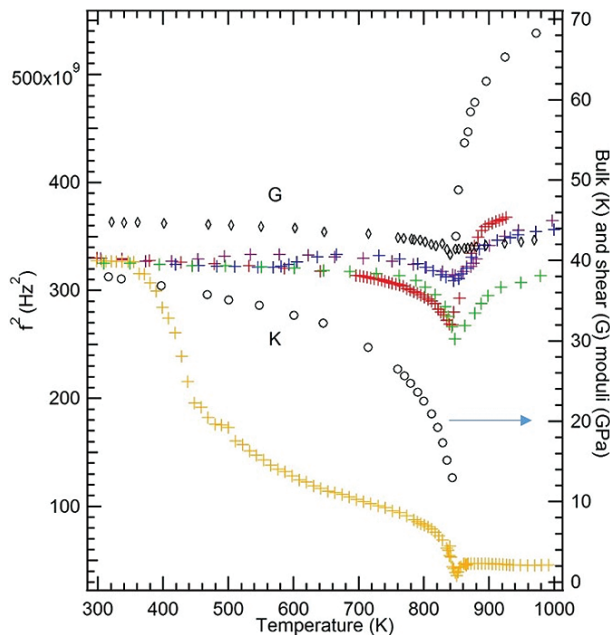


FIGURE 10. Squared frequency variation for Ardownie agate (+), novaculite (+), Brazilian agate (+) (McKnight et al. 2008), Mexican agate (+) (McKnight et al. 2008), sandstone first heating (+) (left axis), and bulk (open circle) and shear (diamond) modulus variation for quartz from Voigt-Reuss-Hill averaged values (Ohno et al. 2006) (right axis) between room temperature and 1000 K.

has some preferential orientation for the quartz grains that is inherited from the nucleation of the sample at low temperatures.

IMPLICATIONS

Porosity of agate, novaculite, and sandstone may, in principle, increase the mechanical response to an applied electric field. It is possible that flexoelectricity, a coupling between polarization and strain gradient, can break the local symmetry (Zubko et al. 2013). Though the flexoelectric effect is generally expected to be weak, Tagantsev et al. (2012) showed that the contribution of surface piezoelectricity to the flexoelectric response of a sample is comparable to that of the static bulk contribution. High porosity then implies larger surface vibrations and hence higher RPS signals. Nevertheless, we see no such effect in Vycor, which has the largest specific surface area, but no piezoelectricity so that the RPS signals seen in this study seem only marginally influenced by flexoelectricity near surfaces.

ACKNOWLEDGMENTS

RUS facilities in Cambridge were established through grant no. NE/B505738/1 to M.A.C. from the Natural Environment Research Council. E.K.H.S. is grateful to the Leverhulme Foundation (RPG-2012-564) and EPSRC (EP/K009702/1) for financial support.

REFERENCES CITED

Aktas, O., Salje, E.K.H., and Carpenter, M.A. (2013a) Polar precursor ordering in BaTiO₃ detected by resonant piezoelectric spectroscopy. *Applied Physics Letters*, 103, 142902.
Aktas, O., Salje, E.K.H., Crossley, S., Lapronti, G.I., Whatmore, R.W., Mathur, N.D., and Carpenter, M.A. (2013b) Ferroelectric precursor behaviour in PbSc_{0.5}Ta_{0.5}O₃ detected by field-induced resonant piezoelectric spectroscopy. *Physical Review B*, 88, 174112.

Baro, J., Corral, A., Illa, X., Planes, A., Salje, E.K.H., Schranz, W., Soto-Parra, D.E., and Vives, E. (2013) Statistical similarity between the compression of a porous material and earthquakes. *Physical Review Letters*, 110, 088702.
Calleja, M., Dove, M.T., and Salje, E.K.H. (2001) Anisotropic ionic transport in quartz: the effect of twin boundaries. *Journal of Physics: Condensed Matter*, 13, 9445–9454.
Carpenter, M.A., Salje, E.K.H., Graeme-Barber, A., Wruck, B., Dove, M.T., and Knight, K.S. (1998) Calibration of excess thermodynamic properties and elastic constant variations associated with the $\alpha \leftrightarrow \beta$ phase transition in quartz. *American Mineralogist*, 83, 2–22.
Damjanovic, D. (1997) Stress and frequency dependence of the direct piezoelectric effect in ferroelectric ceramics. *Journal of Applied Physics*, 82, 1788–1797.
——— (1998) Ferroelectric, dielectric and piezoelectric properties of ferroelectric thin films and ceramics. *Reports on Progress in Physics*, 61, 1267–1324.
Damjanovic, D., Biancoli, A., Batooli, L., Vahabzadeh, A., and Trodhal, J. (2012) Elastic, dielectric and piezoelectric anomalies and Raman spectroscopy of 0.5Ba(Ti_{0.8}Zr_{0.2})O₃-0.5(Ba_{0.7}Ca_{0.3})TiO₃. *Applied Physics Letters*, 100, 192907.
Delenne, J.-Y., Topin, V., and Radjai, F. (2009) Failure of cemented granular materials under simple compression—Experiments and numerical simulations. *Acta Mechanica*, 205, 9–21.
Friend, P.F., Harland, W.B., and Hudson, J.D. (1963) The Old Red Sandstone and the Highland Boundary in Arran, Scotland. *Transactions of the Edinburgh Geological Society*, 19, 363–425.
Keller, W.D., Stone, C.G., and Hoersch, A.L. (1985) Textures of Paleozoic chert and novaculite in the Ouachita Mountains of Arkansas and Oklahoma and their geological significance. *Geological Society of America Bulletin*, 96, 1353–1363.
Levitz, P., Ehret, G., Sinha, S.K., and Drake, J.M. (1991) Porous Vycor glass: The microstructure as probed by electron microscopy, direct energy transfer, small-angle scattering and molecular adsorption. *Journal of Chemical Physics*, 95, 6151–6161.
McKnight, R.E.A., Moxon, T., Buckley, A., Taylor, P.A., Darling, T.W., and Carpenter, M.A. (2008) Grain size dependence of elastic anomalies accompanying the $\alpha \leftrightarrow \beta$ phase transition in polycrystalline quartz. *Journal of Physics: Condensed Matter*, 20, 75–83.
Migliori, A., and Maynard, J.D. (2005) Implementation of a modern resonant ultrasound spectroscopy system for the measurement of the elastic moduli of small solid specimens. *Review of Scientific Instruments*, 76, 121301.
Migliori, A., and Sarrao, J.L. (1997) *Resonant Ultrasound Spectroscopy*, 201 p. Wiley, New York.
Ohno, I., Harada, K., and Yoshitomi, C. (2006) Temperature variation of elastic constants of quartz across the α - β transition. *Physics and Chemistry of Minerals*, 33, 1–9.
Pertsev, N.A., and Salje, E.K.H. (2000) Thermodynamics of pseudoproper and improper ferroelastic inclusions and polycrystals: Effect of elastic clamping on phase transitions. *Physical Review B*, 61, 902–908.
Rios, S., Salje, E.K.H., and Redfern, S.A.T. (2001) Nanoquartz vs. macroquartz: a study of the $\alpha \leftrightarrow \beta$ phase transition. *European Physical Journal B*, 20, 75–83.
Rojac, T., Bencan, A., Drazic, G., Kosec, M., and Damjanovic, D. (2012) Piezoelectric nonlinearity and frequency dispersion of the direct piezoelectric response of BiFeO₃ ceramics. *Journal of Applied Physics*, 112, 064114.
Salje, E.K.H., Ridgwell, A., Guttler, B., Wruck, B., Dove, M.T., and Dolino, G. (1992) On the displacive character of the phase transition in quartz—a hard-mode spectroscopy study. *Journal of Physics: Condensed Matter*, 4, 571–577.
Salje, E.K.H., Koppensteiner, J., Schranz, W., and Fritsch, E. (2010) Elastic instabilities in dry, mesoporous minerals and their relevance to geological applications. *Mineralogical Magazine*, 74, 341–350.
Salje, E.K.H., Soto-Parra, D.E., Planes, A., Vives, E., Reinecker, M., and Schranz, W. (2011) Failure mechanism in porous materials under compression: crackling noise in mesoporous SiO₂. *Philosophical Magazine Letters*, 91, 554–560.
Salje, E.K.H., Aktas, O., Carpenter, M.A., Laguta, V.V., and Scott, J.F. (2013) Domains within domains and walls within walls: Evidence for polar domains in cryogenic SrTiO₃. *Physical Review Letters*, 111, 247603.
Tagantsev, A.K., and Yurkov, A.S. (2012) Flexoelectric effect in finite samples. *Journal of Applied Physics*, 112, 044103.
Vacche, S.D., Oliveira, F., Leterrier, Y., Michaud, V., Damjanovic, D., and Månson J.-A.E. (2012) The effect of processing conditions on the morphology, thermo-mechanical, dielectric, and piezoelectric properties of P(VDF-TrFE)/BaTiO₃ composites. *Journal of Materials Science*, 47, 4763–4774.
Zubko, P., Catalan, G., and Tagantsev, A.K. (2013) Flexoelectric effect in solids. *Annual Review of Materials Research*, 43, 387–421.

MANUSCRIPT RECEIVED AUGUST 29, 2014

MANUSCRIPT ACCEPTED NOVEMBER 30, 2014

MANUSCRIPT HANDLED BY HONGWU XU